

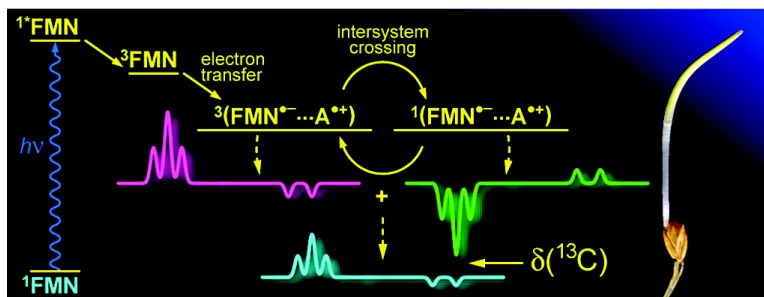
Article

**Photochemically Induced Dynamic Nuclear Polarization in a C450A Mutant of the LOV2 Domain of the *Avena sativa* Blue-Light Receptor Phototropin**

Gerald Richter, Stefan Weber, Werner Rmisch, Adelbert Bacher, Markus Fischer, and Wolfgang Eisenreich

*J. Am. Chem. Soc.*, **2005**, 127 (49), 17245-17252 • DOI: 10.1021/ja053785n • Publication Date (Web): 18 November 2005

Downloaded from <http://pubs.acs.org> on March 25, 2009



**More About This Article**

Additional resources and features associated with this article are available within the HTML version:

- Supporting Information
- Links to the 4 articles that cite this article, as of the time of this article download
- Access to high resolution figures
- Links to articles and content related to this article
- Copyright permission to reproduce figures and/or text from this article

[View the Full Text HTML](#)

## Photochemically Induced Dynamic Nuclear Polarization in a C450A Mutant of the LOV2 Domain of the *Avena sativa* Blue-Light Receptor Phototropin

Gerald Richter,<sup>\*,†,§</sup> Stefan Weber,<sup>\*,‡</sup> Werner Römisch,<sup>†</sup> Adelbert Bacher,<sup>†</sup> Markus Fischer,<sup>†</sup> and Wolfgang Eisenreich<sup>\*,†</sup>

*Technische Universität München, Lehrstuhl für Organische Chemie und Biochemie, Lichtenbergstrasse 4, 85747 Garching, Germany, and Freie Universität Berlin, Fachbereich Physik, Arnimallee 14, 14195 Berlin, Germany*

Received June 9, 2005; E-mail: wolfgang.eisenreich@ch.tum.de; Stefan.Weber@physik.fu-berlin.de; G.Richter@exeter.ac.uk

**Abstract:** Phototropin is a blue-light receptor involved in the phototropic response of higher plants. The photoreceptor comprises a protein kinase domain and two structurally similar flavin-mononucleotide (FMN) binding domains designated LOV1 and LOV2. Blue-light irradiation of recombinant LOV2 domains induces the formation of a covalent adduct of the thiol group of a functional cysteine in the cofactor-binding pocket to C(4a) of the FMN. Cysteine-to-alanine mutants of LOV domains are unable to form that adduct but generate an FMN radical upon illumination. The recombinant C450A mutant of the LOV2 domain of *Avena sativa* phototropin was reconstituted with universally and site-selectively <sup>13</sup>C-labeled FMN and the <sup>13</sup>C NMR signals were unequivocally assigned. <sup>13</sup>C NMR spectra were acquired in darkness and under blue-light irradiation. The chemical shifts and the coupling patterns of the signals were not affected by irradiation. However, under blue-light exposure, exceptionally strong nuclear-spin polarization was developed in the resonances belonging to certain carbons of the FMN's isoalloxazine moiety. An enhancement of the NMR absorption was observed for the signals of C(5a), C(7), and C(9). NMR lines in emission were detected for the signals belonging to C(2), C(4), C(4a), C(6), C(8), and C(9a). The signal of C(10a) remained in absorption but was slightly attenuated. In contrast, the intensities of the NMR signals belonging to the carbons of the ribityl side chain of FMN were not affected by light. The observation of spin-polarized <sup>13</sup>C-nuclei in the NMR spectra of the mutant LOV2 domain is clear evidence for radical-pair intermediates in the reaction steps following optical sample excitation.

### Introduction

The phototropic response of higher plants is mediated by the blue-light receptor phototropin.<sup>1,2</sup> The protein specified by the *phot1* gene<sup>3</sup> comprises a protein kinase domain and two topologically similar domains carrying noncovalently bound FMN chromophores.<sup>4</sup> Blue-light irradiation of the recombinant LOV2 domain (*M* = 12.5 kDa) of *Avena sativa* phototropin causes reversible bleaching of the absorption in the range of 400–500 nm,<sup>4</sup> accompanied by the appearance of absorption at 370 nm to 390 nm attributed to the reversible addition of the thiol group of cysteine-450 to C(4a) of the FMN chromophore (see Figure 1) on the basis of <sup>13</sup>C NMR spectroscopy.<sup>5</sup> A subsequent X-ray diffraction structural analysis of the respective

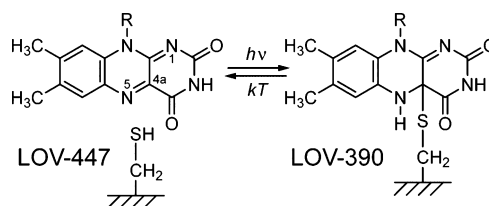


**Figure 1.** Photocycle of wild-type LOV domains. R denotes the ribityl side chain of FMN.

LOV2 domain of *Adiantum capillus-veneris* has confirmed the earlier NMR findings and revealed an FMN chromophore with its isoalloxazine ring strongly deviating from planarity at C(4a) in the light form.<sup>6</sup> The photoadduct undergoes spontaneous fragmentation in the dark with a rate constant of  $2.55 \times 10^{-2} \text{ s}^{-1}$  at room temperature.<sup>7</sup>

The flavin triplet state (<sup>3</sup>FMN) has been proposed as a reactive intermediate in the primary blue-light induced reaction of LOV domains.<sup>8</sup> More specifically, <sup>3</sup>FMN has been suggested to be

<sup>†</sup> Technische Universität München.

<sup>‡</sup> Freie Universität Berlin.

<sup>§</sup> Present address: University of Exeter, School of Biological and Chemical Sciences, Stocker Road, Exeter EX4 4QD, United Kingdom, E-Mail: G.Richter@exeter.ac.uk.

(1) Briggs, W. R.; Christie, J. M. *Trends Plant Sci.* **2002**, *7*, 204–210.

(2) Kagawa, T. *J. Plant Res.* **2003**, *116*, 77–82.

(3) Briggs, W. R. et al. *Plant Cell* **2001**, *13*, 993–997.

(4) Christie, J. M.; Salomon, M.; Nozue, K.; Wada, M.; Briggs, W. R. *Proc. Natl. Acad. Sci. U.S.A.* **1999**, *96*, 8779–8783.

(5) Salomon, M.; Eisenreich, W.; Dürr, H.; Schleicher, E.; Knieb, E.; Massey, V.; Rüdiger, W.; Müller, F.; Bacher, A.; Richter, G. *Proc. Natl. Acad. Sci. U.S.A.* **2001**, *98*, 12357–12361.

(6) Crosson, S.; Moffat, K. *Plant Cell* **2002**, *14*, 1067–1075.

(7) Salomon, M.; Christie, J. M.; Knieb, E.; Lempert, U.; Briggs, W. R. *Biochemistry* **2000**, *39*, 9401–9410.

(8) Swartz, T. E.; Corchnoy, S. B.; Christie, J. M.; Lewis, J. W.; Szundi, I.; Briggs, W. R.; Bogomolni, R. A. *J. Biol. Chem.* **2001**, *276*, 36493–36500.

generated via intersystem crossing (ISC) from an excited singlet-state precursor,<sup>9</sup> and to decay within a few microseconds by generating the FMN-cysteinyl photoadduct.<sup>7</sup> The primary photoreaction has been claimed to proceed (i) via an ionic mechanism,<sup>8</sup> or (ii), in close analogy to the photooxidation of amino acids by <sup>3</sup>FMN,<sup>10</sup> via a radical-pair mechanism with a triplet-configured radical pair converting to a singlet-configured radical pair as a precursor for covalent-bond formation.<sup>11,12</sup> A wealth of information was obtained from LOV mutants in which the functional cysteine was replaced by alanine, serine or methionine.<sup>11,13,14</sup> The Cys → Ala and Cys → Ser mutants do not form covalent adducts but rather undergo spontaneous photoreduction of the FMN chromophore, which is initially in the fully oxidized redox state,<sup>7</sup> to form a one-electron reduced FMN radical.

In this study we present NMR experiments on the LOV2 C450A mutant of *A. sativa* phototropin in which the FMN chromophore has been replaced with universally or specifically <sup>13</sup>C-labeled FMN isotopologs. We report for the first time the observation of photochemically induced dynamic nuclear polarization (photo-CIDNP) in an integral cofactor-protein system probed by solution NMR. A semiquantitative analysis of the polarization phenomenon provides information on the generation of nuclear-spin polarization in the LOV2 mutant domain.

## Experimental Procedures

**Materials.** [U-<sup>13</sup>C<sub>17</sub>]Riboflavin was prepared by fermentation of a riboflavin-producing *Bacillus subtilis* strain using [U-<sup>13</sup>C<sub>6</sub>]-glucose as carbon source.<sup>15</sup> Other <sup>13</sup>C-labeled riboflavin isotopologs were prepared by chemical or enzyme-assisted synthesis.<sup>15–18</sup>

The preparation of the recombinant LOV2 C450A domain (amino acid residues 405 to 559) of *A. sativa* phototropin and its reconstitution with isotope-labeled FMN follows procedures that have been reported elsewhere;<sup>5</sup> for details, cf. Supporting Information.

**NMR Spectroscopy.** NMR spectra were measured at 27 °C using a four-channel DRX-500 spectrometer (Bruker, Karlsruhe, Germany) equipped with a pulsed-field gradient accessory. <sup>13</sup>C NMR spectra were recorded at 125.8 MHz using a 5-mm <sup>1</sup>H/<sup>13</sup>C dual probehead. <sup>13</sup>C chemical shifts were referenced to internal dioxane (67.84 ppm relative to tetramethylsilane, TMS). The solvent contained 25 mM sodium/potassium phosphate, pH 7, 10% (v/v) <sup>2</sup>H<sub>2</sub>O, and 0.5–1 mM protein; the sample volume was 0.5 mL.

Composite pulse decoupling was used. All spectra were recorded using a flip angle of 30°. The repetition rate was 3 s.

Free-induction decays were processed using exponential multiplication. The acquisition of the spectra required 5–20 h.

When required, the samples were irradiated inside the magnet via an optical fiber whose conical tip was immersed into the solution of the NMR tube (15 mm above the magnetic center). The light source was a mercury lamp (Oriol Corporation, Stamford, CT) operating at a constant power of 100 W. The emitted light was filtered using a pair of BG7 and GG420 filters from Schott (Mainz, Germany). Alternatively, a blue-light emitting photodiode (455 nm, 175 mW, Luxeon Star/O Batwing, Lumileds Lighting, San Jose, CA) was used as a light source.

**DFT Computations.** Density-functional computations were performed using the program package Gaussian03.<sup>19</sup> Two different paramagnetic forms of 7,8,10-trimethyl isoalloxazine were tested as models for an FMN radical: (i) a neutral radical form, FIH•, protonated at N(5), and (ii) an anion radical form, FI<sup>•-</sup>, deprotonated at N(5). The geometries of both molecules were optimized using the B3LYP functional and the 6-31G\* basis set. Subsequently, single-point calculations of the unpaired electron-spin density were performed on the optimized structures using the B3LYP functional and the EPR-II basis set. Iso-spin-density surfaces were obtained using the MOLDEN program package.<sup>20</sup>

## Results

The recombinant mutant LOV2 C450A domain used in this study has absorbance maxima at 363 and 447 nm characteristic of an FMN chromophore in the fully oxidized redox state.<sup>7</sup> After blue-light irradiation, the protein shows absorption maxima at 570 and 605 nm (data not shown) as is typical for FMN-radical formation. Photoreduction of this LOV2 mutant has been reported previously to occur in the presence and absence (as is the case in the present study) of exogenous electron donors.<sup>11</sup> In all samples investigated, the flavin radical is completely reoxidized in the dark on a time scale of minutes.

<sup>13</sup>C NMR spectra from LOV2 mutant protein that had been reconstituted with various <sup>13</sup>C-labeled FMN samples were recorded in the dark and under continuous blue-light irradiation (see Figure 2) as described earlier.<sup>5</sup> NMR spectra obtained in the dark and after preliminary irradiation followed by spontaneous reversal to the fully oxidized redox state were essentially identical with the spectra of unirradiated protein. Notably, the signals of the FMN chromophore were not affected. However, some irreversible photodamage was noticed after prolonged sample irradiation as evidenced by a decrease in the signal-to-noise ratio and by the appearance of spurious peaks, albeit of

- (9) Kennis, J. T. M.; Crosson, S.; Gauden, M.; van Stokkum, I. H. M.; Moffat, K.; van Grondelle, R. *Biochemistry* **2003**, *42*, 3385–3392.
- (10) Heelis, P. F.; Parsons, B. J.; Phillips, G. O. *Biochim. Biophys. Acta* **1979**, *587*, 455–462.
- (11) Kay, C. W. M.; Schleicher, E.; Kuppig, A.; Hofner, H.; Rüdiger, W.; Schleicher, M.; Fischer, M.; Bacher, A.; Weber, S.; Richter, G. *J. Biol. Chem.* **2003**, *278*, 10973–10982.
- (12) Schleicher, E.; Kowalczyk, R. M.; Kay, C. W. M.; Hegemann, P.; Bacher, A.; Fischer, M.; Bittl, R.; Richter, G.; Weber, S. *J. Am. Chem. Soc.* **2004**, *126*, 11067–11076.
- (13) Bittl, R.; Kay, C. W. M.; Weber, S.; Hegemann, P. *Biochemistry* **2003**, *42*, 8506–8512.
- (14) Kottke, T.; Dick, B.; Fedorov, R.; Schlichting, I.; Deutzmann, R.; Hegemann, P. *Biochemistry* **2003**, *42*, 9854–9862.
- (15) Römisch, W.; Eisenreich, W.; Richter, G.; Bacher, A. *J. Org. Chem.* **2002**, *67*, 8890–8894.
- (16) Sedlmaier, H.; Müller, F.; Keller, P. J.; Bacher, A. *Z. Naturforsch. C* **1987**, *42*, 425–429.
- (17) van Schagen, C. G.; Müller, F. *Eur. J. Biochem.* **1981**, *120*, 33–39.

- (18) Dwyer, T. M.; Mortl, S.; Kemter, K.; Bacher, A.; Fauq, A.; Frerman, F. E. *Biochemistry* **1999**, *38*, 9735–9745.
- (19) Frisch, M. J.; Trucks, G. W.; Schlegel, H. B.; Scuseria, G. E.; Robb, M. A.; Cheeseman, J. R.; Montgomery, J. A., Jr.; Vreven, T.; Kudin, K. N.; Burant, J. C.; Millam, J. M.; Iyengar, S. S.; Tomasi, J.; Barone, V.; Mennucci, B.; Cossi, M.; Scalmani, G.; Rega, N.; Petersson, G. A.; Nakatsuji, H.; Hada, M.; Ehara, M.; Toyota, K.; Fukuda, R.; Hasegawa, J.; Ishida, M.; Nakajima, T.; Honda, Y.; Kitao, O.; Nakai, H.; Klene, M.; Li, X.; Knox, J. E.; Hratchian, H. P.; Cross, J. B.; Bakken, V.; Adamo, C.; Jaramillo, J.; Gomperts, R.; Stratmann, R. E.; Yazyev, O.; Austin, A. J.; Cammi, R.; Pomelli, C.; Ochterski, J. W.; Ayala, P. Y.; Morokuma, K.; Voth, G. A.; Salvador, P.; Dannenberg, J. J.; Zakrzewski, V. G.; Dapprich, S.; Daniels, A. D.; Strain, M. C.; Farkas, O.; Malick, D. K.; Rabuck, A. D.; Raghavachari, K.; Foresman, J. B.; Ortiz, J. V.; Cui, Q.; Baboul, A. G.; Clifford, S.; Cioslowski, J.; Stefanow, B. B.; Liu, G.; Liashenko, A.; Piskorz, P.; Komaromi, I.; Martin, R. L.; Fox, D. J.; Keith, T.; Al-Laham, M. A.; Peng, C. Y.; Nanayakkara, A.; Challacombe, M.; Gill, P. M. W.; Johnson, B.; Chen, W.; Wong, M. W.; Gonzalez, C.; Pople, J. A. *Gaussian 03*, revision B.04; Gaussian, Inc.: Wallingford, CT, 2004.
- (20) Schaftenaar, G.; Noordik, J. H. *J. Comput.-Aided Mol. Design* **2000**, *14*, 123–134.

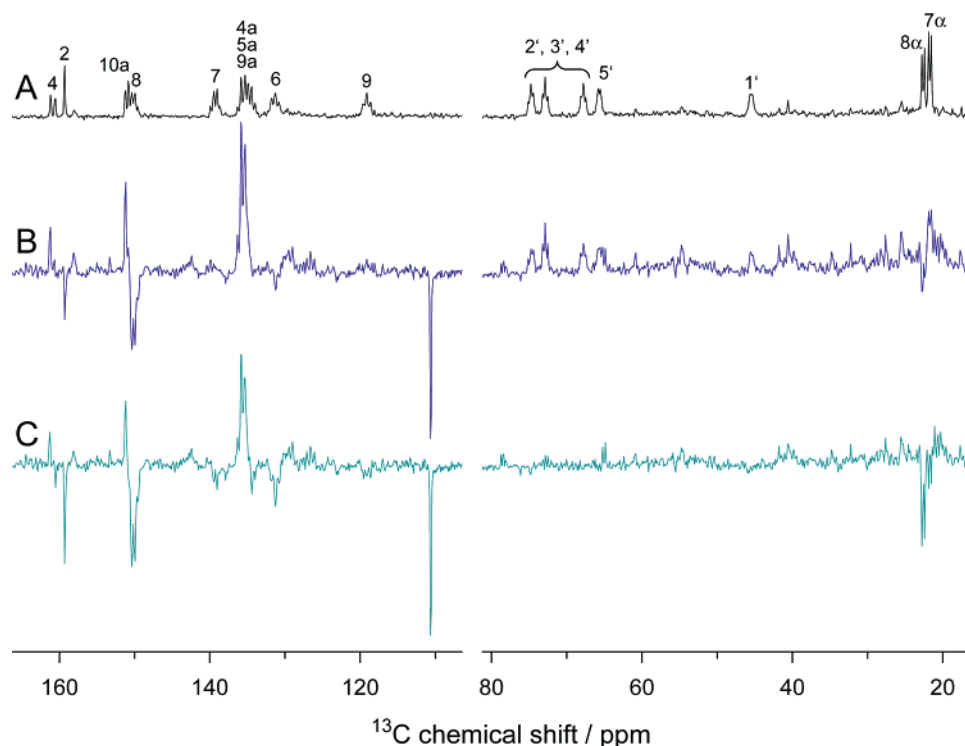


**Figure 2.**  $^{13}\text{C}$  NMR spectra of  $[\text{U}-^{13}\text{C}_{17}]$ FMN-reconstituted LOV2 C450A domain. (A) “Dark” spectrum. (B) Scaled “light” spectrum. (C) Difference spectrum “light”-minus-“dark”.

relatively low intensity. Hence, to avoid photodamage, spectra recorded during illumination were collected with fewer acquisitions as compared to the respective “dark” spectra. The signal-to-noise ratios of the NMR spectra of illuminated samples are therefore typically slightly lower than those of the previously recorded spectra of the protein in the dark.

In the NMR spectra of recombinant LOV2 C450A domains recorded in the dark, most of the  $^{13}\text{C}$ -enriched carbon atoms of the FMN chromophore appear as multiplets in the protein reconstituted with  $[\text{U}-^{13}\text{C}_{17}]$ FMN (Figure 2), and as singlets in protein specimens reconstituted with FMN isotopologs carrying either one or two  $^{13}\text{C}$  atoms (Figure 3).

The NMR line widths of signals from protein-bound FMN were large as compared to those arising from free FMN. A comparison of the chemical shifts of FMN carbons in wild type and in mutant LOV domains reveals only minor differences (see Table in Supporting Information). Apparently, the replacement of C450 by alanine does not significantly alter the surroundings of the FMN chromophore.

On the basis of isotopolog editing using single-labeled and double-labeled FMN in conjunction with the coupling patterns in samples containing  $[\text{U}-^{13}\text{C}_{17}]$ FMN, all  $^{13}\text{C}$  NMR signals of FMN in the LOV2 domain could be unequivocally assigned. Specifically, C(2) appears as a singlet in the spectrum of the protein reconstituted with  $[\text{U}-^{13}\text{C}_{17}]$ FMN. The carbons C(4), C(7 $\alpha$ ), C(8 $\alpha$ ), C(10 $\alpha$ ), C(1'), and C(5') appear as doublets with splittings arising from the spin–spin coupling to the respective neighboring  $^{13}\text{C}$  atoms. Due to simultaneous coupling to two adjacent  $^{13}\text{C}$  atoms, the carbons C(6), C(9), C(2'), C(3'), and C(4') appear as pseudo-triplets. Pseudo-quartets are observed for the carbons C(7) and C(8) due to simultaneous coupling to three directly adjacent  $^{13}\text{C}$  atoms. The multiplet signals of C(4 $\alpha$ ), C(5 $\alpha$ ) and C(9 $\alpha$ ) overlap in the NMR spectra of the LOV2

domain reconstituted with  $[\text{U}-^{13}\text{C}_{17}]$ FMN as their chemical shifts are closely similar. Likewise, the multiplets of C(8) and C(10 $\alpha$ ) overlap.

Blue-light illumination of the protein samples, which results in partial formation of the radical form of FMN, did not affect the chemical shifts of individual carbon atoms (see Figures 2 and 3). Surprisingly, however, some of the signals now appeared with negative signal amplitude, whereas other signals remained in absorption, either with attenuated or enhanced intensity. With the exception of the signal intensities for carbons C(2'), C(3'), C(4'), and C(5') of the ribityl side chain, the intensity ratios between signals measured in the dark or under blue-light condition varied over a wide range. Using the integrals of the ribityl signals as a measure of the amount of diamagnetic (fully oxidized) FMN, we obtain an approximately 3-fold decreased concentration of fully oxidized FMN under light conditions as compared to the sample examined in the dark. Hence, we conclude that the majority of the initially diamagnetic LOV2 domains rests in paramagnetic states in which the individual  $^{13}\text{C}$  NMR signals are broadened beyond detectability due to the strong hyperfine interaction of the nuclear spins with the unpaired electron spin which is mainly located on the FMN's isoalloxazine ring. This conclusion is consistent with the UV–vis spectrum of the sample recorded upon photoexcitation and also with our previous EPR observations of an FMN radical generated by blue-light irradiation of LOV2 C450A.<sup>11</sup>

A difference NMR spectrum (trace C of Figure 2) is obtained by subtracting the spectrum measured under dark conditions (trace A of Figure 2) from the spectrum recorded during illumination that has been scaled such that the signal intensities of the carbons C(2'), C(3'), C(4'), and C(5') match those from the “dark” state (trace B of Figure 2). In this representation, strongly enhanced absorptive polarization of the nuclear spins

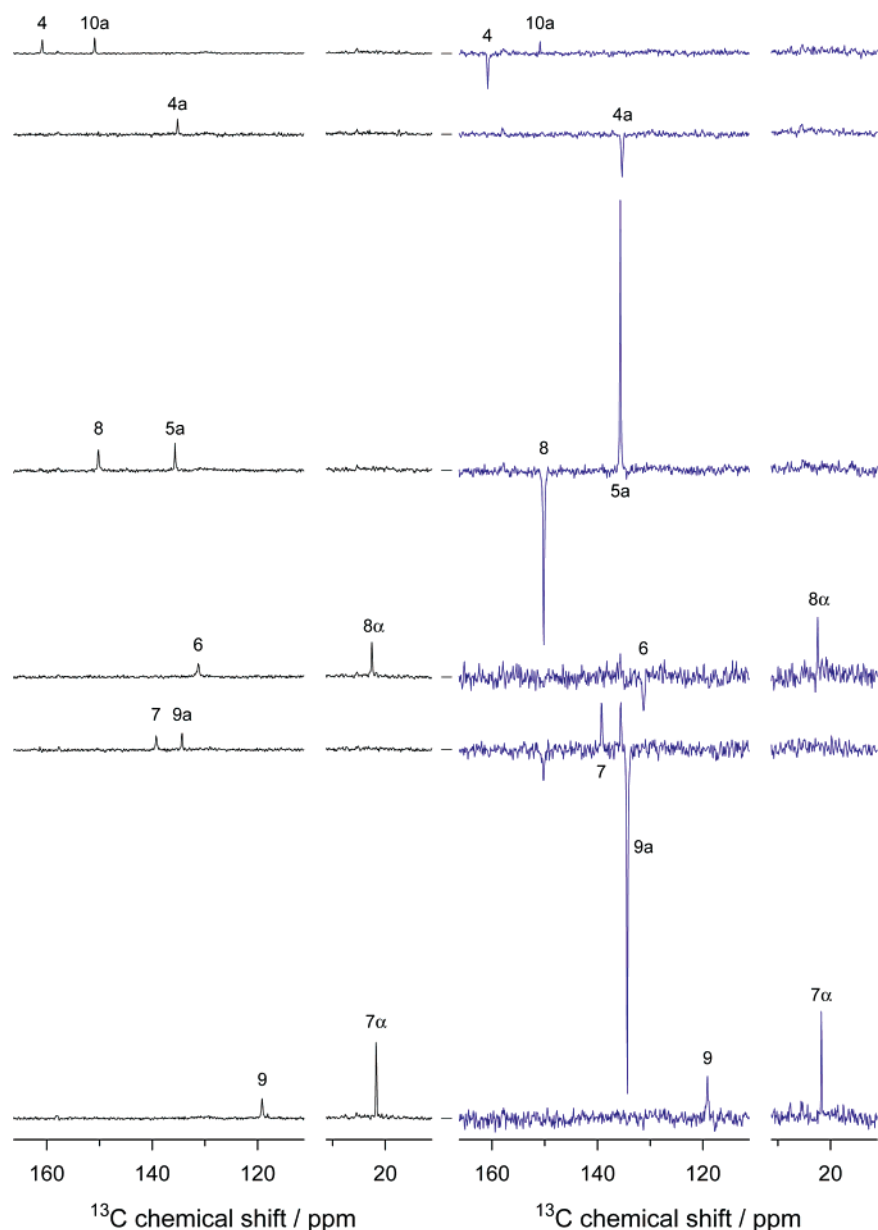


**Figure 3.**  $^{13}\text{C}$  NMR spectra of LOV2 C450A domains reconstituted (from top to bottom) with  $[4,10a\text{-}^{13}\text{C}_2]\text{FMN}$  (first row),  $[4a\text{-}^{13}\text{C}_1]\text{FMN}$  (second row),  $[5a,8\text{-}^{13}\text{C}_2]\text{FMN}$  (third row),  $[6,8\alpha\text{-}^{13}\text{C}_2]\text{FMN}$  (fourth row),  $[7,9a\text{-}^{13}\text{C}_2]\text{FMN}$  (fifth row) and  $[7\alpha,9\text{-}^{13}\text{C}_2]\text{FMN}$  (sixth row). Left column: “dark” spectra. Right column: “light” spectra. For details see text.

is observed in the region where the resonances of C(4a), C(5a), and C(9a) occur. Strong emissive spin polarization is obtained for C(2) and C(8). The multiplet signal assigned to C(6) is weakly emissively polarized. Additionally, a strong emissive NMR line is observed around 110.6 ppm. This signal is not due to the resonance of any of the carbons within the FMN chromophore as it is not observed in the NMR spectrum recorded in the dark. Hence, we conclude that it must be assigned to a  $^{13}\text{C}$  atom situated in the C450A apo-protein, although the amino acid carbon atoms are not  $^{13}\text{C}$ -enriched. Apparently, the signal of this atom becomes strongly polarized as a result of the photoreaction of the mutant domain (see below). There is a notion of other polarized NMR signals in the range between 120 and 140 ppm that are observed when the sample is exposed to blue light but are absent in the dark. These are of weaker intensity than the 110.6-ppm line and some of them are in emission and others in absorption.

For a semiquantitative analysis of the nuclear-spin polarization phenomenon observed in the light reaction of the LOV2 C450A domain, additional NMR experiments were performed with protein samples, in which the flavin cofactor was selectively labeled with one or two  $^{13}\text{C}$  nuclei. The NMR-data analysis of these samples is simpler due to the lack of  $^{13}\text{C}$ – $^{13}\text{C}$  nuclear spin interactions that lead to multiplet signals in LOV2 C450A containing universally labeled FMN. Furthermore, the polarizations of the  $^{13}\text{C}$  NMR signals are easier to discern due to the absence of spectral overlap observed for C(4a), C(5a), and C(9a) as well as for C(8) and C(10a), and C(7 $\alpha$ ) and C(8 $\alpha$ ) in spectra with protein containing  $[\text{U}\text{-}^{13}\text{C}_{17}]\text{FMN}$ .

Spectra recorded under illumination (“light” spectra) are compared to the corresponding “dark” spectra in the right-hand column of Figure 3. All “light” spectra have been scaled using the same scaling factor that was used to compensate for the decreasing amount of fully oxidized (diamagnetic) FMN present

under illumination conditions in the protein reconstituted with [U- $^{13}\text{C}_{17}$ ]FMN. Whereas the chemical shifts of the individual carbon atoms are not affected by illumination, the signal intensities are strongly modulated in the “light” spectra as compared to those obtained in the dark. From the signals due to  $^{13}\text{C}$  atoms in the pyrimidine ring of the isoalloxazine moiety, C(4) and C(4a) reverse their sign during sample irradiation, and the signal of C(10a) becomes slightly attenuated as compared to that obtained in the dark. Very strong polarization changes are predominantly observed for carbons situated in the benzene ring of the isoalloxazine moiety. Specifically, the signals of the carbons C(6), C(8), and C(9a) change their sign from absorptive to emissive. The carbons C(5a), C(9), and C(7) remain in absorption but become slightly more intense. Only small changes in the NMR signal amplitudes are observed for the absorptively polarized carbons C(7 $\alpha$ ) and C(8 $\alpha$ ). Note, however, that in the “light” spectrum of LOV2 C450A containing [U- $^{13}\text{C}_{17}$ ]FMN the carbon C(8 $\alpha$ ) is emissively polarized thus suggesting that cross-polarization<sup>21–23</sup> which transfers magnetization from the strongly emissive polarized  $^{13}\text{C}$ (8) to the directly adjacent  $^{13}\text{C}$ (8 $\alpha$ ) plays an important role in the uniformly  $^{13}\text{C}$ -labeled sample. Such polarization transfer effects are negligible in protein samples reconstituted with FMN isotopologs carrying either only one  $^{13}\text{C}$  or two  $^{13}\text{C}$  nuclei that are not at close distance.

According to the radical-pair theory of photochemically induced nuclear-spin polarization,<sup>24,25</sup> the net polarizations of the NMR lines depend on the electron–nuclear hyperfine couplings which in turn are derived from the unpaired electron-spin density on the individual halves of an intermediate radical pair. Therefore, we performed quantum-chemical calculations on a 7,8,10-trimethyl isoalloxazine radical, which serves as a model for the FMN radical in LOV2. The truncation of the ribityl side chain is justified as the spin densities on the carbons C(2'), C(3'), C(4'), and C(5') and consequently also their hyperfine couplings are negligibly small. Two protonation states have been considered: (i) the anion radical form,  $\text{Fl}^{\bullet-}$  which is deprotonated at N(5) (see Figure 4A), and (ii) the neutral radical form,  $\text{FlH}^{\bullet}$ , with a protonated N(5) atom (see Figure 4B). The amplitudes of the unpaired electron-spin densities of  $\text{Fl}^{\bullet-}$  and  $\text{FlH}^{\bullet}$  in the respective highest-occupied molecular orbital are shown as iso-surfaces, where the blue and red colors represent positive and negative electron-spin density, respectively. Overall, both radical species have a closely similar electron-spin density distribution: positive values are obtained for the carbons C(4), C(4a), C(6), C(8), and C(9a), and negative values are obtained for C(5a), C(7), and C(9). The observed differences at position C(10a) are in agreement with recent quantum-chemical calculations:<sup>26,27</sup> negative spin-density is observed in  $\text{Fl}^{\bullet-}$ , whereas a positive value is obtained at the corresponding position in  $\text{FlH}^{\bullet}$ . Furthermore, the negative spin densities at C(5a), C(7), and C(9) are higher in amplitude in the anion radical when compared to the neutral radical.

From analyses of the NMR spectra of LOV2 C450A samples containing selectively  $^{13}\text{C}$ -labeled FMN, two types of amplitude

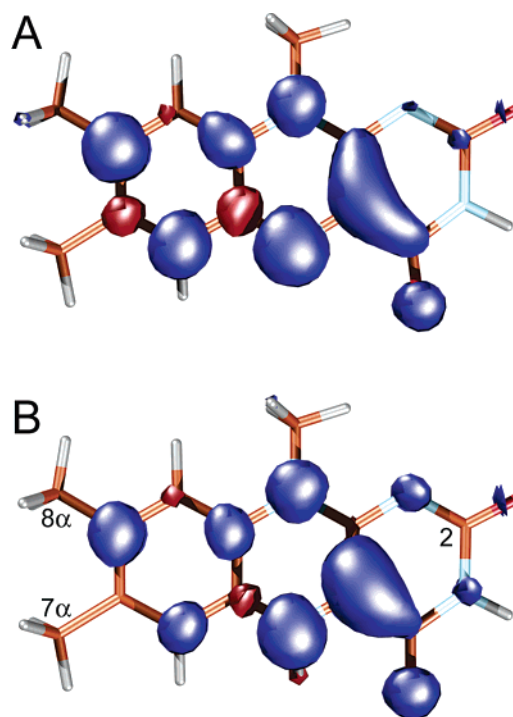


**Figure 4.** Density-functional calculations of the unpaired electron-spin density in a flavin anion radical,  $\text{Fl}^{\bullet-}$  (A), and a neutral radical,  $\text{FlH}^{\bullet}$  (B).

changes are observed when comparing “dark” and “light” states: NMR signals that change the polarization from absorptive to emissive or that are attenuated but still in absorption in the presence of light have been assigned to atoms C(2), C(4), C(4a), C(6), C(8), C(9a), and C(10a). Absorptive signals that are enhanced originate from the atoms C(5a), C(7), and C(9). According to Kaptein’s rules for the polarization of NMR lines,<sup>24</sup> these two groups of nuclei must then have hyperfine couplings of opposite sign. If we assume (in considering the results from quantum-chemical calculations of hyperfine couplings)<sup>26,27</sup> that emissive and enhanced absorptive polarized NMR lines arise from carbons with positive and negative hyperfine couplings, respectively, we then obtain a hyperfine pattern that correlates with the FMN anion radical,  $\text{FMN}^{\bullet-}$ , rather than with the neutral FMN radical,  $\text{FMNH}^{\bullet}$ . Hence, we conclude that the nuclear spin-dependent mixing of singlet and triplet states is more likely to take place in the anionic rather than in the neutral radical state.

## Discussion

Polarized NMR transitions are a signature of CIDNP, a phenomenon which has been first observed more than 35 years ago in products of photoinduced radical reactions.<sup>28,29</sup> The term CIDNP refers to non-Boltzmann nuclear spin-state distributions detected as enhanced absorptive or emissive NMR signals. The origin of CIDNP lies in the radical-pair mechanism which postulates that if the outcome of a photochemical reaction depends on the extent of singlet–triplet mixing in the radical-pair intermediates and if this mixing is partly driven by the electron–nuclear hyperfine interaction, then the reaction prod-

(21) Closs, G. L.; Czeropski, M. S. *Chem. Phys. Lett.* **1977**, *45*, 115–116.  
 (22) De Kanter, F. J. J.; Kaptein, R. *Chem. Phys. Lett.* **1979**, *62*, 421–426.  
 (23) Hore, P. J.; Egmond, M. R.; Edzes, H. T.; Kaptein, R. *J. Magn. Reson.* **1982**, *49*, 122–150.  
 (24) Kaptein, R. *Adv. Free Rad. Chem.* **1975**, *5*, 319–380.  
 (25) Closs, G. L. *Chemically Induced Dynamic Nuclear Polarization*; Academic Press: New York, 1974; Vol. 7.

(26) Weber, S.; Möbius, K.; Richter, G.; Kay, C. W. M. *J. Am. Chem. Soc.* **2001**, *123*, 3790–3798.  
 (27) García, J. I.; Medina, M.; Sancho, J.; Alonso, P. J.; Gómez-Moreno, C.; Mayoral, J. A.; Martínez, J. I. *J. Phys. Chem. A* **2002**, *106*, 4729–4735.  
 (28) Bargon, J.; Fischer, H. Z. *Naturforsch.* **1967**, *22A*, 1556–1562.  
 (29) Ward, H. R.; Lawler, R. G. *J. Am. Chem. Soc.* **1967**, *89*, 5518–5519.

ucts could have strongly polarized NMR lines.<sup>24,30–32</sup> Despite the fact that CIDNP was extended with great success to biopolymers<sup>33,34</sup> and is nowadays used as a technique to probe the surface structure and folding of proteins using exogenous photosensitizers to induce radical-pair reactions,<sup>34–36</sup> photo-CIDNP in integral protein–cofactor systems has so far only been observed in photosynthetic reaction centers of bacteria<sup>37–39</sup> and plants.<sup>40,41</sup> These protein complexes, however, are so large that solid-state NMR techniques such as magic-angle spinning need to be applied to obtain narrow NMR signals. The details of the mechanism of producing photo-CIDNP in the solid state are currently under discussion.<sup>42,43</sup> Although a variety of flavoproteins were examined earlier in the search of nuclear polarization effects, in no case they have been observed without adding either “external” flavins, or redox-active amino acids such as tryptophan or tyrosine.<sup>44</sup>

Nuclear-spin polarization in solution NMR arises from the remarkable fact that the spin state of magnetic nuclei may influence chemical reactivity. The spin-sorting process in a radical-pair reaction does not necessarily need to be very efficient to nevertheless lead to strong enhancements of NMR intensities. A potential reaction mechanism for the origin of nuclear polarization in the LOV2 C450A protein is required to be consistent with our present findings as well as with recent observations of an FMN radical in this protein: (i) Strong triplet populations in wild-type and mutant LOV2 have been observed by time-resolved optical spectroscopy<sup>8</sup> and EPR.<sup>12</sup> This is indicative of a high quantum yield for triplet formation via ISC. (ii) Compared to NMR spectra obtained from LOV2 C450A in the dark, strongly polarized signals in enhanced absorption and emission are observed when NMR spectra are recorded in the presence of blue light. (iii) While the intensities of the individual <sup>13</sup>C NMR signals of FMN in LOV2 C450A strongly depend on the irradiation conditions, the chemical shift values of the NMR resonances are unchanged when comparing “dark” and “light” spectra. Therefore, we conclude that both the unpolarized NMR lines recorded in the dark and the polarized NMR lines obtained in the presence of blue light originate from <sup>13</sup>C nuclei in FMN of the same (diamagnetic) fully oxidized redox state. (iv) If the integrated signal intensities of the carbons in the ribityl side chain of FMN are taken as a measure for the amount of fully oxidized FMN in [U-<sup>13</sup>C<sub>17</sub>]FMN-containing samples, then a considerably decreased amount of FMN in this redox state is detected under blue-light illumination. (v) In the “light” spectra,

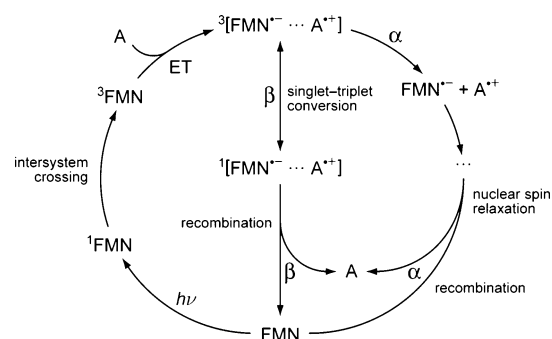


**Figure 5.** Proposed cyclic reaction scheme for the production of photo-CIDNP in LOV2 C450A. A is a redox-active amino acid side-chain in the protein.  $\alpha$  and  $\beta$  denote the nuclear-spin state(s) of a <sup>13</sup>C nucleus in FMN and A (for details, see text).

an additional strongly emissive NMR line at 110.6 ppm and some more weakly polarized lines in the range between 120 and 140 ppm are observed. These signals cannot be assigned to any of the carbons in the FMN chromophore and hence must originate from spin-polarized <sup>13</sup>C nuclei (occurring at natural abundance) in the apoprotein. (vi) The observed NMR-intensity modulations that distinguish the “dark” and “light” spectra correlate with the electron-spin density distribution of an FMN anion radical, FMN<sup>•-</sup>. On the other hand, a neutral radical (FMNH<sup>•</sup>) in LOV2 C450A has been detected by optical spectroscopy and EPR (see below).<sup>11</sup> The lifetime of this radical was determined to be in the range of several minutes to hours depending on the presence or absence of oxygen and/or exogenous reductants.

In Figure 5 we present a cyclic reaction scheme that is consistent with the above-mentioned experimental observations. This scheme originally proposed by Kaptein has previously been applied to rationalize the production of nuclear-spin polarization in the photosensitized reaction of exogenous FMN with surface-exposed redox-active amino acid residues in proteins.<sup>33,35</sup> The ground-state FMN in the fully oxidized (diamagnetic, and hence NMR-observable) redox state is promoted into its excited singlet state, <sup>1</sup>FMN, by absorption of blue light. This is followed by ISC to the triplet state, <sup>3</sup>FMN, which is generated with high quantum yield. <sup>3</sup>FMN is a potent oxidant for redox-active amino acid residues within the LOV2 domain, and may thus abstract an electron from a nearby redox-active amino acid residue (species A in Figure 5) to form a geminate radical pair, <sup>3</sup>[FMN<sup>•-</sup> ... A<sup>•+</sup>], in a spin-correlated triplet electron-spin configuration. If the distance between the two radical-pair halves is too close (less than about 1 nm), then the electron–electron exchange interaction would be too large to permit triplet-to-singlet interconversion. However, if the radicals are well separated (and hence the exchange interaction, and in rigid systems also the dipolar interaction, are comparable in size to the isotropic hyperfine couplings), then hyperfine interactions may induce triplet-to-singlet interconversion in the radical-pair state. The initially generated triplet radical pair has then two possible fates: (i) <sup>3</sup>[FMN<sup>•-</sup> ... A<sup>•+</sup>] may either evolve into an electronic singlet state, <sup>1</sup>[FMN<sup>•-</sup> ... A<sup>•+</sup>], which subsequently may undergo spin-allowed back electron transfer to regenerate the ground-state reactants (FMN and A), or (ii) so-called escape products are formed directly from <sup>3</sup>[FMN<sup>•-</sup> ... A<sup>•+</sup>] because radical recombination is spin-forbidden from the triplet spin configuration. If we assume that the frequency of the coherent

- (30) Closs, G. L. *J. Am. Chem. Soc.* **1969**, *91*, 4552–4554.  
 (31) Lawler, R. G. *J. Am. Chem. Soc.* **1967**, *89*, 5519–5521.  
 (32) Lawler, R. G. *Acc. Chem. Res.* **1972**, *5*, 25–33.  
 (33) Hore, P. J.; Broadhurst, R. W. *Prog. Nucl. Magn. Reson. Spectrosc.* **1993**, *25*, 345–402.  
 (34) Hore, P. J.; Winder, S. L.; Roberts, C. H.; Dobson, C. M. *J. Am. Chem. Soc.* **1997**, *119*, 5049–5050.  
 (35) Mok, K. H.; Hore, P. J. *Methods* **2004**, *34*, 75–87.  
 (36) Maeda, K.; Lyon, C. E.; Lopez, J. J.; Cemazar, M.; Dobson, C. M.; Hore, P. J. *J. Biomol. NMR* **2000**, *16*, 235–244.  
 (37) Zysmilich, M. G.; McDermott, A. *J. Am. Chem. Soc.* **1994**, *116*, 8362–8363.  
 (38) Zysmilich, M. G.; McDermott, A. *Proc. Natl. Acad. Sci. U.S.A.* **1996**, *93*, 6857–6860.  
 (39) Zysmilich, M. G.; McDermott, A. *J. Am. Chem. Soc.* **1996**, *118*, 5867–5873.  
 (40) Alia; Roy, E.; Gast, P.; van Gorkom, H. J.; de Groot, H. J. M.; Jeschke, G.; Matysik, J. *J. Am. Chem. Soc.* **2004**, *126*, 12819–12826.  
 (41) Matysik, J.; Alia; Gast, P.; van Gorkom, H. J.; Hoff, A. J.; de Groot, H. J. M. *Proc. Natl. Acad. Sci. USA* **2000**, *97*, 9865–9870.  
 (42) Polenova, T.; McDermott, A. *J. Phys. Chem. B* **1999**, *103*, 535–548.  
 (43) Jeschke, G.; Matysik, J. *Chem. Phys.* **2003**, *294*, 239–255.  
 (44) Müller, F.; van Schagen, C. G.; Kaptein, R. *Methods Enzymol.* **1980**, *66*, 385–416.

interconversion of singlet and triplet radical-pair states depends on the spin state of the  $^{13}\text{C}$  nuclei in the FMN chromophore via the electron–nuclear hyperfine interaction, and if we (arbitrarily) further suppose that this interconversion is faster when one (or several)  $^{13}\text{C}$  atoms are in a  $\beta$ -spin state ( $m_I = -1/2$ ), then triplet radical pairs containing  $^{13}\text{C}$  in the  $\beta$  configuration are more likely to cross over to the singlet state and recombine (see Figure 5). On the other hand, triplet radical pairs containing the same carbons in the opposite spin configuration ( $\alpha$ , i.e.,  $m_I = +1/2$ ) are then more likely to yield uncorrelated radicals as escape products. These may ultimately also recombine to regenerate the same ground-state reactants, FMN and A, thus leading to a cancellation of the opposite recombination and escape nuclear polarizations unless the recombination reaction of the free radicals is considerably slower than geminate recombination from  $^1[\text{FMN}^{\bullet-}\cdots\text{A}^{\bullet+}]$  as is typically the case. In LOV2 C450A, radical recombination takes place on a time scale of minutes depending on the experimental conditions.<sup>11</sup> Hence, under the influence of the unpaired electron spins, nuclear spin–lattice relaxation in the escape products is expected to be faster than radical recombination, thus leading to an appreciable reduction of the nuclear-spin polarization generated via the  $^3[\text{FMN}^{\bullet-}\cdots\text{A}^{\bullet+}]$  channel. Consequently, complete cancellation of the recombination and escape nuclear polarizations is averted as a result of nuclear spin–lattice relaxation in the one path leading to FMN and A via recombination of the escape products. Note that translational diffusion (an inherent property of the photo-CIDNP mechanism of photoreactions of low-molecular-weight substances) of one or both radicals of the radical-pair state is not required as a prerequisite for the observation of NMR polarizations in integral-cofactor proteins as long as the exchange and dipolar electron–electron interactions in the precursor radical-pair state are not too large, and two distinct pathways exist where the opposite nuclear-spin polarizations resulting from singlet–triplet conversion can progress differently. While the nuclear-spin polarization phenomenon in LOV2 C450A can be described by the radical-pair mechanism outlined above, we cannot presently exclude that other mechanisms, such as a triplet mechanism,<sup>45</sup> contribute (at least in part) to the polarization of the NMR lines of FMN. However, the observation of nuclear-spin polarized NMR transitions derived from a counter radical ( $\text{A}^{\bullet+}$  in Figure 5) leads us to the conclusion that a triplet-based mechanism can only play a minor role in the present system.

In the radical-pair reaction scheme described above, the polarized NMR line at 110.6 ppm and the other more weakly polarized lines in the 120–140-ppm range stem from a redox-active amino acid, A, that acts as an electron donor to  $^3\text{FMN}$ . In photo-CIDNP studies on the solvent accessibility of proteins using exogenously added FMN as photosensitizer, typically tyrosine, tryptophan or histidine radicals are observed.<sup>35,44</sup> The appearance of a signal with a chemical shift of 110.6 ppm in our experiments is suggestive of a tryptophan residue, where C(3) (IUPAC numbering scheme for the indole side group of tryptophan; see Figure in Supporting Information) of the aromatic side chain typically resonates at 109 to 112 ppm downfield from TMS as has been shown for tryptophan in a variety of proteins<sup>46,47</sup> and model compounds.<sup>47</sup> This is also the

carbon that carries the highest (positive) electron-spin density (0.556) in the neutral radical state.<sup>48</sup> Using DFT, a large and positive isotropic hyperfine-coupling constant of 1.58 mT with pronounced dipolar anisotropy has been calculated for  $^{13}\text{C}(3)$ . More than 2-fold lower spin densities and hence smaller hyperfine couplings have been calculated for the other carbons in the tryptophan indole ring. Specifically, electron-spin densities of  $-0.105$ ,  $0.194$ ,  $0.151$ , and  $0.063$ , and isotropic hyperfine coupling constants of  $-0.8$  mT,  $0.53$  mT,  $0.36$  mT, and  $0.02$  mT, have been computed for C(3a), C(4), C(6), and C(7a), respectively.<sup>48</sup> In the high-magnetic-field limit ( $|\Delta g B_0| \gg |A_i|$ , where  $\Delta g$  is the  $g$ -value difference  $g(\text{FMN}^{\bullet-}) - g(\text{A}^{\bullet+})$ ,  $B_0$  is the magnetic field, and  $A_i$  is the hyperfine coupling constant of a nucleus  $i$ ), the nuclear-spin polarization of a nucleus should be roughly proportional to its isotropic hyperfine coupling constant in the radical state. Hence, the NMR signals of C(3a), C(4), C(6), and C(7a) are expected to show considerably weaker nuclear-spin polarization than C(3) but should nevertheless be observed in the “light” spectra. That the polarization of C(3) is overwhelmingly strong could be due to differences in the nuclear spin–lattice relaxation times of the various nuclei that determine the degree of cancellation of recombination and escape polarizations. Slow relaxation in the diamagnetic ground state in combination with fast relaxation in the radical states of FMN and the amino acid residue A leads to a reduced cancellation of the opposite escape and recombination polarizations. The quarternary carbons C(3), C(3a), and C(7a) of the aromatic side chain of tryptophan exhibit long relaxation times in the diamagnetic ground state of tryptophan as compared to the other  $^{13}\text{C}$  nuclei. In the radical state, however, the relaxation times of these nuclei might be quite different. If nuclear-spin relaxation is governed by hyperfine anisotropies due to molecular tumbling of A, then C(3) will have fast relaxation due to the large anisotropy of its hyperfine coupling, whereas C(3a) and C(7a) will show slower relaxation due to their smaller hyperfine anisotropy. This will then lead to enhanced cancellation of recombination and escape polarizations in C(3a) and C(7a) as compared to C(3). In combination with the continuous sample illumination, the large net polarization of C(3) in A could be further enhanced through repetitive sample excitation leading to a delicate balance of CIDNP pumping and decay.

In the LOV2 domain under examination, there are two tryptophans, W491 and W557, which are both well separated ( $>1.3$  nm in a calculated structure of *A. sativa* LOV2 C450A based on *Adiantum* LOV2<sup>49</sup> as a model) from the FMN chromophore thus fulfilling the requirements for the generation of nuclear-spin polarization governed by nuclear hyperfine interactions. Future point-mutational studies are aimed at an unambiguous identification of the amino acid interacting with FMN in a photoinitiated radical-pair mechanism.

To summarize, we have for the first time observed nuclear polarization effects in an integral protein using solution  $^{13}\text{C}$  NMR. From a prospective quantitative analysis of the polarization phenomenon under standardized illumination conditions, valuable information on the electronic structure of paramagnetic intermediate states in LOV domains will be obtained through the nuclear-spin polarization that is detected in the diamagnetic reaction products. We expect that this method is widely

(45) Stehlik, D. *Excited States* **1977**, 3, 203–303.

(46) Eisenreich, W.; Bacher, A. *J. Biol. Chem.* **1991**, 266, 23840–23849.

(47) Sun, H.; Oldfield, E. *J. Am. Chem. Soc.* **2004**, 126, 4726–4734.

(48) Himo, F.; Eriksson, L. A. *J. Phys. Chem. B* **1997**, 101, 9811–9819.

(49) Crosson, S.; Moffat, K. *Proc. Natl. Acad. Sci. U.S.A.* **2001**, 98, 2995–3000.



applicable to other medium-sized flavoproteins as well, to unravel electron-transfer pathways and to identify the redox partners involved in the protein function.

**Acknowledgment.** We thank Professor Peter J. Hore (University of Oxford) for very helpful discussions and comments on this manuscript. This study was supported by grants from the Deutsche Forschungsgemeinschaft (SFB 498, project B7, and SFB 533, project A5) and the Volkswagen Stiftung (grant I/77100). We also thank Mrs. Ulrike Stier (Bad Soden) and the

Hans Fischer Gesellschaft e.V. for generous sponsoring of this research work.

**Supporting Information Available:** Experimental details; one Table with  $^{13}\text{C}$  NMR chemical shifts of free FMN, FMN bound to *Avena sativa* LOV2, and FMN bound to *Avena sativa* LOV2 C450A; one Figure with IUPAC numbering scheme of tryptophan; complete Ref. (3); complete Ref. (19). This material is available free of charge via the Internet at <http://pubs.acs.org>.  
JA053785N